EUROPEAN ORGANIZATION FOR NUCLEAR RESEARCH

L3 Internal Note 2329

September 21st, 1998

SEARCHES FOR GLUEBALL CANDIDATES IN $\gamma\gamma$ COLLISIONS AT LEP AND CESR

Alvise Favara

Presented at the 29th International Conference on High Energy Physics, Vancouver, July 22–30, 1998.

SEARCHES FOR GLUEBALL CANDIDATES IN $\gamma\gamma$ COLLISIONS AT LEP AND CESR

ALVISE FAVARA

California Institute of Technology, HEP 256–48, Pasadena, CA 91125, USA
also at
CERN, EP, 1211 Geneva 23, Switzerland
E-mail: Alvise.Favara@cern.ch

Recent results on resonance formation in $\gamma\gamma$ collisions are presented. Searches for the two best glueball candidates, the $f_0(1500)$ and the $f_J(2220)$, in the $\pi^+\pi^-$ and in the $K^0_S K^0_S$ channels are reviewed. No evidence for the $f_0(1500)$ or the $f_J(2220)$ signal is reported and new compelling upper limits, at 95% C.L., on their $\Gamma_{\gamma\gamma}$ are set. These limits support the interpretation of the $f_0(1500)$ and the $f_J(2220)$ in terms of gluon bound states.

1 Introduction

Quantum Chromodynamics (QCD) is, by now, a well established theory for the description of strong interactions between quarks and gluons. Many experimental confirmations of this theory have been obtained in the high energy regime as well as in hadron spectroscopy.

The distinctive feature of QCD as a non-Abelian gauge theory is the self-interaction of gluons. Indirect experimental evidence of this fact has been obtained from the study of multi-jet events in experiments at high energy colliders. Yet the main consequence of self-interactions among gluons is the existence of a new form of matter [1], called glueball, which is a bound state of two or more gluons. Unfortunately, glueballs have not been identified so far and theoretical predictions in the non-perturbative regime are not precise enough to guide the experimental search.

The discovery of glueballs is heavily related to a complete understanding of the $q\bar{q}$ mass spectrum. Glueball production is expected to be enhanced in gluon rich environments, such as in $p\bar{p}$ and pp collisions and in J/ψ decays, and suppressed in two-photon collisions as gluons have no electric charge.

1.1 Two-photon Collisions

Resonance formation in two-photon collisions follows the scheme shown in Figure 1 and its cross section is given by:

$$\sigma(\gamma^*\gamma^* \to \mathrm{R}) = 8\pi(2J+1)\frac{\Gamma_{\gamma\gamma}\Gamma_R}{(m_R^2 - W_{\gamma\gamma}^2)^2 + m_R^2\Gamma_R^2} \quad (1)$$

where $W_{\gamma\gamma}$ is the two-photon invariant mass, J the spin of the resonance, m_R its mass, $\Gamma_{\gamma\gamma}$ its two-photon width and Γ_R its total width. The two-photon width, being proportional to the fourth power of the constituent quark charges, expresses the flavour content of a resonance. In two-photon collisions, resonances with spin 0 or 2 [a] and with positive C-parity can be produced.

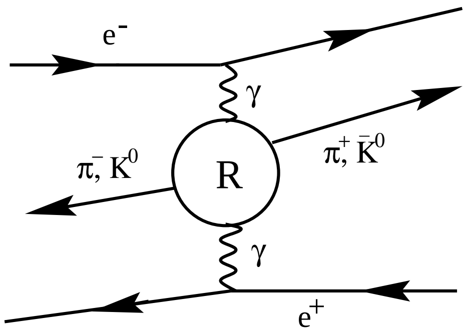

Figure 1: Resonance formation in $\gamma\gamma$ collisions.

The role of two-photon collisions in glueball searches is to anti-tag known resonances. For this purpose a useful glueball figure of merit, called stickiness, is defined [2]. It measures the ratio of the colour charge to the electric charge for a given resonance, R. Its expression is given by:

$$S_R = N_l\left(\frac{m_R}{k_{J/\psi\to\gamma R}}\right)^{2l+1}\frac{\Gamma(J/\psi\to\gamma R)}{\Gamma(R\to\gamma\gamma)} \sim \frac{|<R|gg>|^2}{|<R|\gamma\gamma>|^2} \quad (2)$$

where $\Gamma(R\to\gamma\gamma)$ is the two-photon width, $\Gamma(J/\psi\to\gamma R)$ the J/ψ partial width into γR, m_R and l the mass and spin of the resonance, k the photon energy in $J/\psi \to \gamma R$ decays, and N_l is a normalization factor such that $S_{f_2(1270)} = 1$.

1.2 Scalar and Tensor Meson Nonets

In this paper we report on searches in the $\pi^+\pi^-$ and in the $K^0_S K^0_S$ channels where only scalar and tensor mesons can be observed. According to theoretical predictions [3] based on lattice calculations, the scalar glueball should

[a] Photons are quasi-real if e^+e^- are undetected, hence spin 1 is highly suppressed.

have a mass of 1.6 ± 0.15 GeV, and the tensor glueball a mass of 2.2 ± 0.2 GeV.

A full understanding of the scalar nonet has not yet been achieved. Many broad and interfering resonances in the $1.0 \div 1.5$ GeV region make the identification of the scalar nonet members very difficult. In addition, it is likely that among those resonances the scalar glueball is present. Unfortunately, the glueball state can mix with $q\bar{q}$ states loosing its specific features, like flavour blind couplings. It is still under discussion [4] whether the $s\bar{s}$ state and the scalar glueball have been identified or not. The $s\bar{s}$ state is supposed to be in the region $1.5 \div 1.8$ GeV, while the $f_0(1500)$ is thought to be the scalar glueball [5].

The situation is much cleaner in the tensor nonet where all the members have found their corresponding physical resonance. The anomaly is related to the observation of the $f_J(2220)$, also known as $\xi(2230)$, by Mark III [6] and BES [7], which is probably a spin 2 resonance. The statistical significance of this resonance is now large and its narrow width ($\Gamma \simeq 20$ MeV) as well as its flavour blind couplings suggest an interpretation as the tensor glueball.

2 Searches in the $\pi^+\pi^-$ Final State

2.1 Search for the $f_0(1500)$ *at LEP*

This analysis [8] uses 160.9 pb^{-1} of integrated luminosity collected from 1990 to 1995 at $\sqrt{s} \simeq 91$ GeV with the ALEPH detector. Events in the $\pi^+\pi^-$ channel should satisfy the following criteria: only 2 tracks originating from the interaction point and with opposite charges; small total transverse momentum; small visible energy and mass to reject Z decays; no energy in the forward detectors to select quasi-real photon collisions. In addition muons, electrons and kaons are efficiently rejected by means of the muon chambers and the energy loss measurement in the tracking chamber.

The $\pi^+\pi^-$ invariant mass spectrum for the selected data is shown in Figure 2. This spectrum is used to search for the process $\gamma\gamma \to f_0(1500) \to \pi^+\pi^-$. The clear peak in Figure 2 is due to the $f_2(1270)$. The mass resolution ($\sigma_M \simeq 10$ MeV) and the detection efficiency for the $f_2(1270)$ and the $f_0(1500)$ ($\varepsilon_{f_0(1500)} \simeq 14\%$) are evaluated by means of a Monte Carlo simulation. The background level in the region of the $f_0(1500)$ signal is estimated by extrapolating the fit to the mass spectrum into the region $1.38 \div 1.62$ GeV. The fitted Breit-Wigner parameters for the $f_2(1270)$ are 1211 ± 4 MeV for the mass and 211 ± 18 MeV for the width, revealing a large interference with the $\pi^+\pi^-$ continuum (the PDG [4] values are 1275 ± 1 MeV and 185 ± 4 MeV respectively) which has not been taken into account in the simulation.

No evidence for the $f_0(1500)$ signal is observed. From

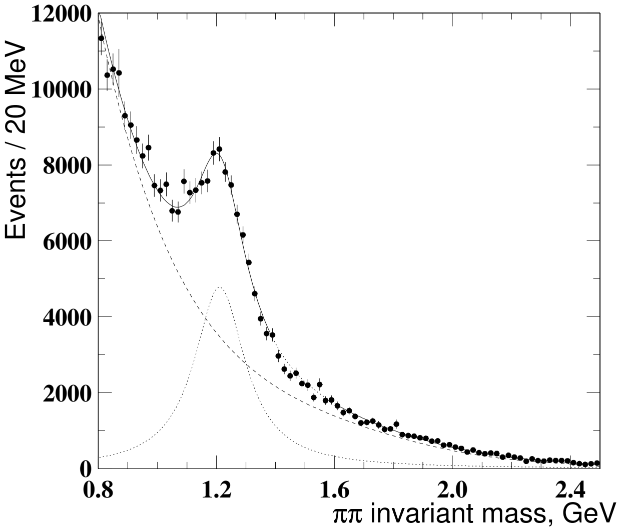

Figure 2: $\pi^+\pi^-$ mass spectrum for the selected data in ALEPH. The fit to the data includes a polynomial for the $\pi^+\pi^-$ continuum and a Breit-Wigner for the $f_2(1270)$.

a likelihood fit in the mass window $1.38 \div 1.62$ GeV, a limit at 95% C.L. is set on $\Gamma_{\gamma\gamma} \times BR(f_0(1500) \to \pi^+\pi^-) < 33.6$ eV. Including also systematic uncertainties, the limit is set to $\Gamma_{\gamma\gamma} < 170$ eV. This value is used to set a lower limit on the stickiness of the $f_0(1500)$: $S_{f_0(1500)} > 13$ at 95% C.L.

2.2 Search for the $f_J(2220)$ *at CESR*

This analysis [9] uses 4.77 fb^{-1} of integrated luminosity collected at $\sqrt{s} \simeq 10.6$ GeV with the CLEO detector. The selection of events from the process $\gamma\gamma \to \pi^+\pi^-$ is very similar to that described in Section 2.1. In this analysis the small visible energy requirement is applied to reject Υ decays.

In order to perform a Monte Carlo simulation of the process $\gamma\gamma \to f_J(2220) \to \pi^+\pi^-$, the $f_J(2220)$ resonance is assumed to have spin 2. For helicity 0, events are in the very forward region and the detection efficiency is only 13.1%, while for helicity 2, events are in the central region and the efficiency is 26.9%. The final efficiency of 24.9% is obtained using a ratio of 1:6 between the two helicity states. The $\pi^+\pi^-$ invariant mass spectrum for the selected data is shown in Figure 3. In the same Figure, the hatched histogram shows the simulated signal distribution, where resolution effects ($\sigma_M \simeq 12$ MeV) are included. The background level in the region of the $f_J(2220)$ signal is estimated by extrapolating the fit to the mass spectrum into the window $2200 \div 2268$ MeV.

No excess over the expected background is observed in the $f_J(2220)$ mass region. In this mass window, a likelihood fit is performed to obtain an upper limit at 95% C.L. of 2.5 eV on $\Gamma_{\gamma\gamma} \times BR(f_J(2220) \to \pi^+\pi^-)$. In

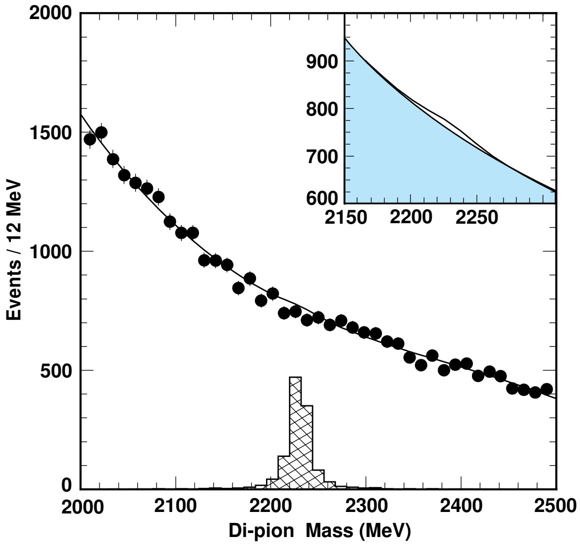

Figure 3: $\pi^+\pi^-$ mass spectrum for the selected data in CLEO. In the insert the two fits: without signal and with the signal yield corresponding to the upper limit.

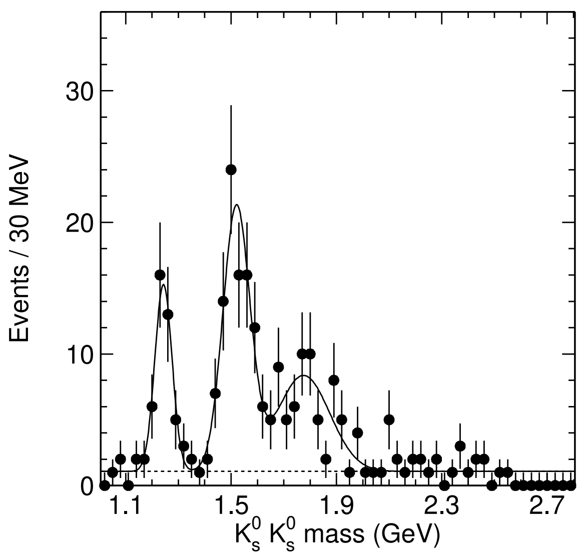

Figure 4: $K^0_S K^0_S$ mass spectrum for the selected data in L3. Three Gaussians, and a constant for the background, are used to fit the peaks of the $f_2(1270) - a_2(1320)$, the $f_2^{'}(1525)$ and the $f_J(1710)$.

this fit, the final signal distribution is the convolution of different signal distributions obtained spanning the mass and the width of the $f_J(2220)$ within their errors. The upper limit on $\Gamma_{\gamma\gamma} \times BR(f_J(2220) \to \pi^+\pi^-)$ is used to set a lower limit on the stickiness of the $f_J(2220)$: $S_{f_J(2220)} > 73$ at 95% C.L.

3 Searches in the $K^0_S K^0_S$ Final State

3.1 Search for the $f_J(2220)$ at LEP

The L3 collaboration presented an analysis [10] of the reaction $\gamma\gamma \to K^0_S K^0_S$, with $K^0_S \to \pi^+\pi^-$, based on 143 pb^{-1} of integrated luminosity at $\sqrt{s} \simeq 91$ GeV and 52 pb^{-1} at $\sqrt{s} \simeq 183$ GeV. The selection is similar to that described in Section 2.1. Events with four charged tracks, small visible energy and small total transverse momentum are selected. In addition the presence of two secondary vertices is required. The final criterion to select a clean sample of K^0_S pairs is $\sum_i (M_{(\pi^+\pi^-)_i} - M_{K^0_S})^2 < (40 \text{ MeV})^2$, where $\sigma_{M_{(\pi^+\pi^-)}} = 9.6$ MeV.

Figure 4 shows the 253 events selected in data from the reaction $\gamma\gamma \to K^0_S K^0_S$, where the background contamination is expected to be negligible. The spectrum is dominated by the $f_2^{'}(1525)$, but a peak at approximately 1250 MeV and an enhancement at approximately 1750 MeV are also clearly visible. No apparent excess is detected in the $f_J(2220)$ mass region.

The small peak at 1250 MeV is the result of the $f_2(1270) - a_2(1320)$ destructive interference, in agreement with the theoretical prediction for the $K^0_S K^0_S$ final state. The enhancement at 1750 MeV could be evidence of the $s\bar{s}$ state of the scalar meson nonet. A firm evidence of this state, which would be strongly coupled to $K\bar{K}$, would support the interpretation of the $f_0(1500)$ as the scalar glueball. From a fit of the spectrum in Figure 4 the mass and the width of the $f_2^{'}(1525)$ and of a second resonance are measured and their values are respectively: 1520 ± 7 MeV and 119 ± 15 MeV, 1770 ± 20 MeV and 200 ± 50 MeV. In the existing spectrum of known resonances, the $f_J(1710)$ is the one which best matches the observation of L3 in the 1750 MeV region. The measured mass and width, and the limited statistics do not allow a firm conclusion, but from now on we will refer to this second peak as the $f_J(1710)$.

According to the Monte Carlo simulation the detection efficiency for the $f_2^{'}(1525)$ is 3.9% for helicity 0 and 7.6% for helicity 2. The theoretical prediction that helicity-2 states should be dominant is verified studying the K^0_S polar angle distribution in the two-photon centre-of-mass system ($\cos\theta^*$). Data events in the selected mass window and Monte Carlo events generated with helicity 2 or helicity 0 hypothesis are compared and the result is shown in Figure 5. The χ^2 values for the two hypotheses are, respectively, 7 and 81 for nine degrees of freedom. This result confirms the prediction that helicity 2 states should be dominant. Using the helicity 2 hypothesis a value of 85 ± 12 eV is obtained for the $\Gamma_{\gamma\gamma} \times BR(f_2^{'}(1525) \to K\bar{K})$.

Even though the statistics for the $f_J(1710)$ are very limited an attempt is made to establish its spin. The $f_J(1710)$ could be a radially excited state of the $f_2^{'}(1525)$ or the $s\bar{s}$ state of the scalar meson nonet. Figure 6 shows the K^0_S polar angle distributions in the two-photon

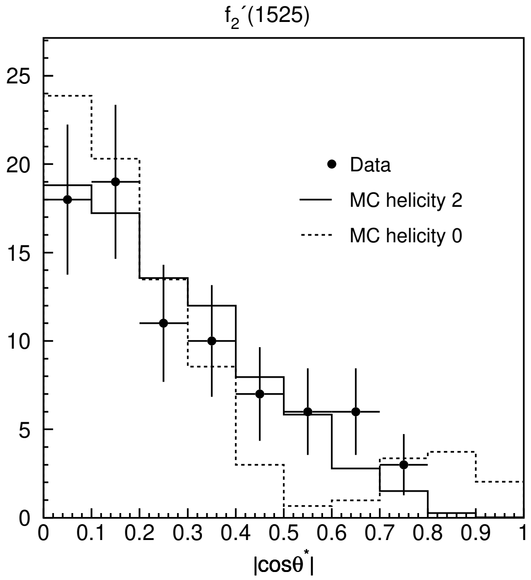

Figure 5: K^0_S polar angle distributions in the two-photon centre-of-mass system, for L3 data and Monte Carlo in the $f_2'(1525)$ mass region.

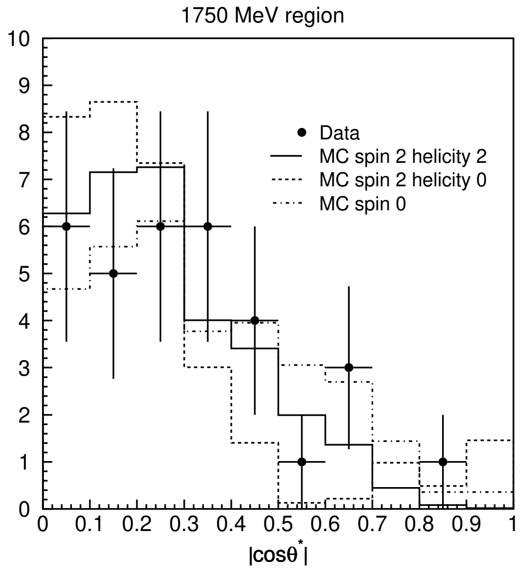

Figure 6: K^0_S polar angle distributions in the two-photon centre-of-mass system, for L3 data and Monte Carlo in the $f_J(1710)$ mass region.

centre-of-mass system for data events in the selected mass window, and for Monte Carlo events generated with spin 2 helicity 2, spin 2 helicity 0 and spin 0. Having χ^2 values of 15, 55 and 6 for nine degrees of freedom, both the spin 2 helicity 2 and the spin 0 interpretations are allowed.

The process $\gamma\gamma \to f_J(2220) \to K^0_S K^0_S$ has been simulated assuming a spin 2 for the $f_J(2220)$ resonance. The detection efficiency for helicity-2 states, which are as-

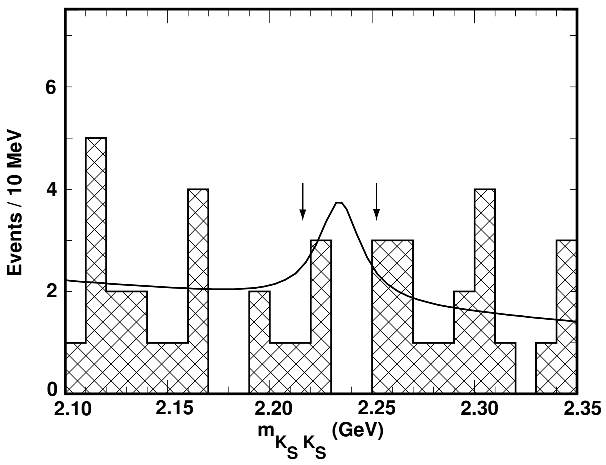

Figure 7: $K^0_S K^0_S$ mass spectrum for the selected data in the $f_J(2220)$ mass region in CLEO. The fit to the data includes the signal yield corresponding to the upper limit.

sumed to be dominant, is 16.5%. The mass resolution for K^0_S pairs is approximately 60 MeV. The upper limit on the production of the $f_J(2220)$ is obtained counting events in the window 2234 ± 120 MeV. The background level is estimated by an extrapolation of the values of the 2σ wide sidebands. The upper limit at 95% C.L. on $\Gamma_{\gamma\gamma} \times BR(f_J(2220) \to K^0_S K^0_S)$ is set at 4.1 eV. This upper limit is converted into a lower limit on the stickiness of the $f_J(2220)$: $S_{f_J(2220)} > 28.6$ at 95% C.L.

3.2 Search for the $f_J(2220)$ *at CESR*

There is a similar analysis [11] performed by CLEO using 3.0 fb^{-1} of integrated luminosity collected at $\sqrt{s} \simeq$ 10.6 GeV. Events from the reaction $\gamma\gamma \to K^0_S K^0_S$, with $K^0_S \to \pi^+\pi^-$, are selected as previously described for the L3 analysis. The main difference is in the $\pi^+\pi^-$ mass requirement, which is $\sum_i (M_{(\pi^+\pi^-)_i} - M_{K^0_S})^2 < (10 \text{ MeV})^2$, where $\sigma_{M_{(\pi^+\pi^-)}} = 3.3$ MeV.

For signal simulation the $f_J(2220)$ is assumed to have spin 2. The detection efficiency for helicity-0 states is 7% while for helicity-2 states is 15%. The final efficiency is obtained according to the ratio 1:6 between the two helicity states. The estimated mass resolution for K^0_S pairs is 9 MeV.

No enhancement over the expected background is observed in the signal mass region shown in Figure 7. The mass window to be considered in the calculation of the upper limit on the production of the $f_J(2220)$, is optimized according to ε^2/b. The efficiency (ε) depends on the $f_J(2220)$ parameters, and the background (b) is evaluated from a fit in the region $2.05 \div 2.35$ GeV excluding 40 MeV around the expected signal mass. The upper limit at 95% C.L. on $\Gamma_{\gamma\gamma} \times BR(f_J(2220) \to K^0_S K^0_S)$ is 1.3 eV. Varying the values of the $f_J(2220)$ parameters by 1σ

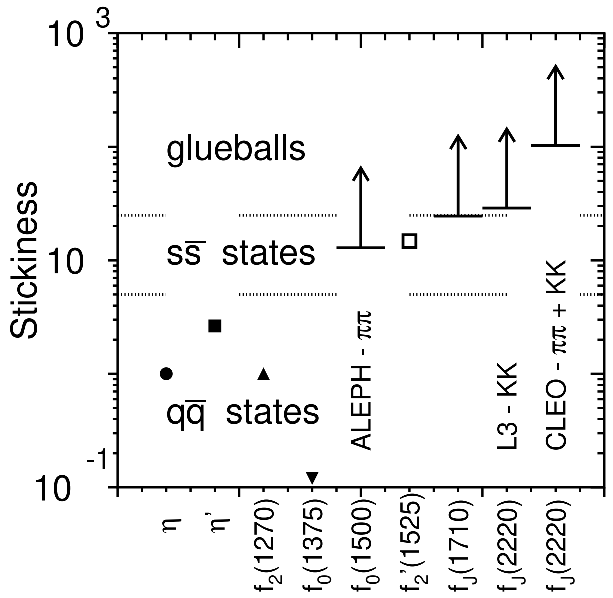

Figure 8: Stickiness values for several resonances. The recent 95% C.L. lower limits from ALEPH, CLEO and L3 are also shown.

this limit can range between 1.2 eV and 1.8 eV. This upper limit is converted into a lower limit on the stickiness of the $f_J(2220)$: $S_{f_J(2220)} > 82$ at 95% C.L.

4 Summary and Conclusions

New results on resonance formation in two-photon collisions have been reviewed. Searches for the scalar glueball candidate $f_0(1500)$ and for the tensor glueball candidate $f_J(2220)$ do not find any evidence for a signal both in the $\pi^+\pi^-$ and in the $K^0_S K^0_S$ final states. In the L3 analysis there may be evidence for an $f_J(1710)$ signal, but this interpretation needs confirmation.

To more clearly identify the glueball nature of a resonance we can combine experimental upper limits on its $\Gamma_{\gamma\gamma}$ with its production rate in J/ψ radiative decays. This combination is expressed in the stickiness, defined in Eq. (2), which is to some extent equivalent to the ratio of the colour charge to the electric charge. Small values of stickiness are expected for mixed $u\bar{u} - d\bar{d}$ mesons. Larger values are expected for pure $s\bar{s}$ states, while even larger values are expected for glueballs which can couple to $\gamma\gamma$ only by creation of a virtual $q\bar{q}$ pair.

Figure 8 shows stickiness values for several resonances. For some resonances only upper limits on $\Gamma_{\gamma\gamma}$ exist, which result in lower limits on the stickiness. In Figure 8 indicative domains for the stickiness of glueballs, $s\bar{s}$ and $q\bar{q}$ states are shown. Resonances like the η and η' are in the $q\bar{q}$ domain, while the $f_2'(1525)$ is thought to be the $s\bar{s}$ state of the tensor meson nonet. So far only upper limits have been published [4] on the $\Gamma_{\gamma\gamma}$ of the $f_J(1710)$, leaving open both the interpretation as the scalar glueball and as the $s\bar{s}$ state of the scalar meson nonet. If the L3 signal can be interpreted as the $f_J(1710)$, this would lead to a stickiness value very close to the present 95% C.L. lower limit, and in agreement with the $s\bar{s}$ state hypothesis. Concerning the two best glueball candidates, the $f_0(1500)$ and the $f_J(2220)$, the new results are summerized below:

- new limit on $S_{f_0(1500)} > 13$ at 95% C.L. by ALEPH
- new limit on $S_{f_J(2220)} > 28.6$ at 95% C.L. by L3
- new limit on $S_{f_J(2220)} > 102$ at 95% C.L. obtained by CLEO combining their analyses of the $\pi^+\pi^-$ and $K^0_S K^0_S$ channels [9].

No firm conclusions can be drawn yet, but there are strong indications that the $f_J(2220)$ is the tensor glueball. Our improved knowledge of the $f_0(1500)$ and the $f_J(1710)$, suggests that the $f_0(1500)$ might be the scalar glueball and the $f_J(1710)$ the scalar $s\bar{s}$ state.

In the coming years LEP will take advantage of an integrated luminosity forty times higher (4 experiments with 500 pb^{-1} each) than that presented in this paper. CLEO as well, will take new data and we can foresee that the final word will be said about glueballs.

References

1. H. Fritzsch *et al.*, *Nuovo Cimento* A **30**, 393 (1975).
2. M. Chanowitz in *VI International Workshop on Photon-Photon Collisions*, ed. R. Lander (World Scientific, Singapore, 1984).
3. G. Bali *et al.*, *Phys. Lett.* B **309**, 378 (1993).
   H. Chen *et al.*, *Nucl. Phys.* B **34**, 357 (1994).
   J. Sexton *et al.*, *Phys. Rev. Lett.* **75**, 4563 (1995).
   A. Szczepaniak *et al.*, *Phys. Rev. Lett.* **76**, 2011 (1996).
4. Particle Data Group, *Eur. Phys. Journal* C **3**, 1 (1998).
5. C. Amsler and F.E. Close, *Phys. Rev.* D **53**, 295 (1996).
6. Mark III Collab., R.M. Baltrusaitis *et al.*, *Phys. Rev. Lett.* **56**, 107 (1986).
7. BES Collab., J.Z. Bai *et al.*, *Phys. Rev. Lett.* **76**, 3502 (1996).
8. ALEPH Collab., R. Barate *et al.*, Contrib. paper 907, ICHEP 98, Vancouver, 1998.
9. CLEO Collab., R. Godang *et al.*, Contrib. paper 872, ICHEP 98, Vancouver, 1998.
10. L3 Collab., M. Acciarri *et al.*, Contrib. paper 522, ICHEP 98, Vancouver, 1998.
11. CLEO Collab., R. Godang *et al.*, *Phys. Rev. Lett.* **79**, 3829 (1997).